Journal of Cleaner Production 184 (2018) 152–159

Contents lists available at ScienceDirect

Journal of Cleaner Production

journal homepage: www.elsevier.com/locate/jclepro

A novel energy consumption model for milling process considering tool wear progression

K.N. Shi [a, 1], D.H. Zhang [a], N. Liu [b, *, 1], S.B. Wang [b], J.X. Ren [a], S.L. Wang [c]

[a] The Key Laboratory of Contemporary Design and Integrated Manufacturing Technology, Ministry of Education, Northwestern Polytechnical University (NPU), Xi'an, Shaanxi 710072, People's Republic of China
[b] Department of Mechanical Engineering, National University of Singapore, 9 Engineering Drive 1, Singapore 117576, Singapore
[c] College of Mechanical Engineering, Chongqing University, Chongqing 400044, People's Republic of China

ARTICLE INFO

Article history:
Received 28 September 2017
Received in revised form
14 December 2017
Accepted 21 February 2018
Available online 22 February 2018

Keywords:
Energy efficiency
Energy consumption modelling
Tool wear
Milling process
Cutting power

ABSTRACT

Energy crisis, climate change, and stringent legislations are imposing great pressure on enterprises, especially manufacturing sectors, to improve their energy efficiency. To achieve higher energy efficiency in manufacturing, reliable energy consumption modelling is the prerequisite since it offers fundamental basis for any energy efficiency-related optimization. Although tool wear is inevitable, traditional energy consumption models fail to take tool wear effects into consideration. To address this issue, this study proposes an energy consumption model with tool wear progression for 3-axis milling process. Based on modern machining theory and recent achievements in energy consumption modelling, the proposed model is firstly derived as an expression with unknown coefficients. Subsequently, the involved coefficients are calibrated based on cutting experiments. With the explicit energy consumption model, power consumption with a given tool wear under new cutting conditions can be predicted with a high accuracy. In addition, as the model reveals a one-to-one correspondence between the power consumption and tool wear, the tool wear can also be effectively estimated from the measured power consumption. Compared with other tool wear monitoring methods such as acoustic emission and vibration, this power consumption-based tool wear estimation method is not only straightforward but also cost-effective. To the best of the authors' knowledge, the proposed energy consumption model with tool wear progression is the first model that was experimentally validated in terms of total power prediction and tool wear prediction, respectively. As such, the proposed model can be a significant supplement to existing energy consumption modelling in machining process, and may provide a more accurate and comprehensive platform for energy efficiency optimization.

© 2018 Elsevier Ltd. All rights reserved.

1. Introduction and literature review

Energy crisis, air pollution and climate change are arousing more and more concerns from all over the world. To address these problems, manufacturing sectors have an important role to play since they are among the largest energy consumers in modern societies (Gutowski and Dahmus, 2007), but with relatively low energy efficiency (Park et al., 2009). Reducing energy consumption in manufacturing enterprises has become one of the most challenging tasks (Li et al., 2017). Improvement in energy efficiency will not only benefit these enterprises economically, but also help to alleviate the aforementioned problems. Therefore, energy-efficient manufacturing has been attracting extensive attention from both industry and academia (Bunse et al., 2011).

In order to achieve higher energy efficiency in manufacturing, especially in discrete parts manufacturing, a thorough understanding of the energy consumption manners in machining processes is the prerequisite (Cai et al., 2017). Over the past decade, numerous studies have made valuable contributions towards reliable and accurate energy consumption modelling/prediction. For example, Gutowski et al. (2006) proposed an energy consumption model as $P = P_{idle} + k \cdot MRR$. In this model, the total power (P) consists of a constant idle part (P_{idle}) and a variable part that is proportional to material removal rate ($k \cdot MRR$). The main problem with this model is the lack of

* Corresponding author.
E-mail addresses: shikaining224@gmail.com (K.N. Shi), liuning@u.nus.edu (N. Liu).
[1] K.N. Shi and N. Liu contribute equally to this study.

https://doi.org/10.1016/j.jclepro.2018.02.239
0959-6526/© 2018 Elsevier Ltd. All rights reserved.

experimental validation. Li and Kara (2011) reported an inverse relationship between the specific energy consumption (*SEC*) and *MRR* in a turning process as $SEC = C_0 + C_1/MRR$, where C_0 and C_1 are constant coefficients. The energy decomposition of machining process was thoroughly investigated in their study. Further, Kara and Li (2011) validated the inverse model in both turning and milling processes. Reported prediction results reached a high accuracy of over 90%. Diaz et al. (2011) modelled the specific energy of a micromachining centre and studied the difference between the power requirements of cutting aluminium and steel. *MRR* is also found to be the most relevant parameter that affects power consumption. Subsequently, Li et al. (2013) extended this inverse model by taking rotation speed (n) into consideration. The improved energy model are proposed as $SEC = k_0 + k_1 n/MRR + k_2/MRR$ with k_0, k_1 and k_2 representing the coefficients. Compared to other major models, this model was more accurate for a milling machine with relatively low standby power. It is worth noticing that most of these models employ empirical modelling methods and consider *MRR* as a unique identifier. However, cutting experiments show that the energy consumption under the same *MRR* is not always the same. This indicates more parameters should be considered in order to better model the energy consumption in machining process. To address this problem, Guo et al. (2012) modelled *SEC* as a function of major cutting parameters, including cutting speed, feedrate, depth of cut and final workpiece diameter. A two-step approach was applied for minimizing cutting parameters in finish turning operations. Similarly, Kuram et al. (2013) modelled the specific cutting energy as a polynomial function of feedrate, depth of cut and cutting speed. Specific energy, surface roughness and tool life were considered as major objectives when optimizing milling parameters and cutting fluid types. Furthermore, undeformed chip thickness was considered by Balogun and Mativenga (2014) when calculating the specific cutting energy. The specific machining energy requirement and its relationship to thickness of material removed were investigated. Recently, Liu et al. (2015) proposed a hybrid energy consumption model for a milling process. The cutting power is analytically calculated, followed by empirically characterization of the relationship between the total power and cutting power. These power models are more comprehensive since more process parameters are considered. However, for these models to work properly, one assumption is required, i.e., the cutter condition, especially the tooltip condition, should remain the same. In fact, material removal in machining process is achieved by the interaction between tooltip and workpiece. According to reported cutting force studies (Budak et al., 1996; Lee and Altintas, 1996), the interaction includes not only cutting, but also rubbing and ploughing. As such, the tooltip will not stay in a static condition. Instead, it will progress dynamically as the machining process continues. For example, Luo et al. (2017) found the effective cutting edge radius may get larger and there may be wear lands on rake/flank tool face. More specifically, Hou et al. (2015) found that tool wear will increase the friction force and press force on unit flank length. Similarly, Sun et al. (2013) also proved that tool wear may cause a substantial increase of the cutting force. In such cases, the aforementioned power consumption models would no longer provide reliable prediction results since the cutting forces required by a worn tool are significantly different from that of a sharp tool. To account for tool wear effects, many studies have been carried out. Valuable information has been provided regarding the tool wear effects on energy consumption in machining processes. For example, Shao et al. (2004) established a cutting power model in face milling process. A tool wear monitoring strategy was also proposed based on threshold power. However, the employed cutting force model with tool wear progression only considered the contribution of flank wear land. In fact, the tool wear happens not only in flank face, but also in rake face and tool tip. Therefore, the contribution of these wear lands should not be overlooked. Besides, only cutting component was considered; rubbing/ploughing component was not involved in the calculation of tangential cutting force. As such, it may lead to inaccurate estimations of the cutting power. In addition, this model focused on cutting power; the relationship between the total power and tool wear was neither studied nor validated quantitatively. Similarly, Yoon et al. (2014) proposed a power consumption model for 3-axis milling process that considered cutting parameters and tool wear. Since the model was obtained using purely empirical method, it failed to predict power consumption with tool wear under new cutting conditions. Sealy et al. (2015) modelled the energy consumption in precision hard milling. They found that tool wear had the greatest influence on net cutting energy consumption. However, this study mainly focuses on qualitative analysis. An explicit expression of the total power with tool wear progression is still lacking. Recently, Liu et al. (2016a) studied the relationships between material removal rate and specific energy, emissions, and environmental impact. The energy consumption of a cutting insert (E_w) is proposed as a function of flank wear (w) is given by $E_w = E_{r0} w/w_c$, where E_{r0} is the embodied energy of a cutter insert and w_c is the critical flank wear. Their study also revealed that tool wear has a significant influence on the energy consumption of milling process. In real production, the proposed model is quite difficult to implement since the embodied energy is usually unavailable. Thus, a more straightforward model is needed to address the tool wear effects.

Motivated by the existing challenges, this study aims to establish an explicit power consumption model as a function of tool wear, major cutting parameters (e.g., feedrate, rotation speed, depth of cut), and properties of tool-workpiece couple (e.g., cutter geometry, cutting force coefficients). This model is firstly derived from theoretical cutting force analysis and makes full use of the hybrid model proposed by Liu et al. (2015). Subsequently, the coefficients in the derived power model were calibrated through a set of cutting experiments. Finally, the obtained explicit power model was validated in cutting experiments under new cutting conditions for power prediction and tool wear prediction, respectively. The study may advance the current state-of-the-art in the following perspectives:

(a) The authors' previous work (Liu et al., 2015) employed a static tooltip condition when predicting the power consumption. In real production, tool wear is inevitable. When tool wear happens, the prediction results given by the previous model are no longer reliable. This study starts from the previous model, and derives a novel model to address tool wear effects. Using a polynomial approximation method, the dynamic condition of the cutter can be effectively modelled. Thus, the proposed model is able to predict energy consumption with tool wear progression.

(b) Compared to Shao et al. (2004), the calculation of cutting power is improved by involving the power due to ploughing/rubbing. More importantly, the overall effects of different wear lands (tool flank, rake face, tool tip, etc.) are considered holistically using a quadratic polynomial approximation method. In addition, the relationship between the total power consumption and tool wear is also derived and subsequently validated in cutting experiments under new cutting conditions.

2. Energy consumption with tool wear progression in 3-axis end milling process

As shown in Fig. 1, the cutting forces in 3-axis milling with a flat-end mill are (Budak et al., 1996; Lee and Altintas, 1996):

$$F_t^0 = \int K_{te}\mathrm{d}S + K_{tc}s_t \sin\psi \mathrm{d}z \tag{1a}$$

$$F_r^0 = \int K_{re}\mathrm{d}S + K_{rc}s_t \sin\psi \mathrm{d}z \tag{1b}$$

$$F_a^0 = \int K_{ae}\mathrm{d}S + K_{ac}s_t \sin\psi \mathrm{d}z \tag{1c}$$

where F_t^0, F_r^0, F_a^0 (N) are the cutting forces in tangential, radial, and axial direction when there is no wear on the tool tip; K_{tc}, K_{rc}, K_{ac} (N/mm^2) and K_{te}, K_{re}, K_{ae} (N/mm) are the specific cutting and edge force coefficients; s_t (mm/rev) is the feed per tooth; ψ (rad) is the radial immersion angle of the current infinitesimal cutting edge; dS (mm) is the length of the current infinitesimal cutting edge; z (mm) is the position of the current infinitesimal cutting edge in axial direction; dz (mm) is the differential length in axial direction. The overall cutting forces are calculated by integrating all the infinitesimal cutting edges engaged in cutting.

According to Waldorf et al. (1992), the effect of the tool flank wear on the cutting force can be modelled by adding a force component normal to the flank wear land and another force component due to friction on the flank wear land. Most of tool wear-related works in the existing literature employed this assumption and modelled the tool wear as an additional friction force. However, the tool wear happens not only in flank face, but also rake face and tool tip. The effects of these wear lands should be considered in a holistic manner. To address this, a polynomial approximation method was employed to model the tool wear effects. Using tool flank wear value ($\overline{VB}$) as a unique indicator, the tangential cutting force are assumed to be

$$F_t(\psi, z, \overline{VB}) = \left[1 + f(\overline{VB})\right] \cdot F_t^0 \tag{2}$$

where $f(\overline{VB})$ is a polynomial function of $\overline{VB}$ that characterizes the increase pattern of the cutting force, as shown in Eq. (3).

$$f(\overline{VB}) = \sum_{i=1}^{N} a_i \overline{VB}^i \tag{3}$$

where a_i are polynomial coefficients. Assuming the tooltip condition can be uniquely indicated by $\overline{VB}$, the cutting force increase pattern versus $\overline{VB}$ should remain the same regardless of the cutting parameters (i.e., the coefficients are constant). This assumption is generally acceptable as long as there is no abrupt tool breakage. It was pointed out by Liu et al. (2015) that spindle rotation contributes to most of the cutting power consumption. Therefore, the cutting power with tool wear progression ($P_{cutting}$) is

$$P_{cutting} \approx \left[1 + f(\overline{VB})\right] F_t^0 V = \left[1 + f(\overline{VB})\right] \cdot P_{cutting}^0 \tag{4}$$

where $P_{cutting}^0$ calculated as $P_{cutting}^0 = \int (K_{te}dS + K_{tc}s_t \sin\psi \mathrm{d}z) \cdot 2\pi nr/60000$ is the cutting power without tool wear; V (m/s) calculated as $V = 2\pi rn/60{,}000$ is the cutting speed with n and r representing the rotation speed (rpm) and cutter radius (mm), respectively. Finally, the total power can be estimated from the calculated cutting power according to the hybrid energy consumption model proposed by Liu et al. (2015) as

$$\begin{aligned} P &= C_1 + C_2\overline{P_{cutting}} = C_1 + C_2\left[1 + f(\overline{VB})\right] \cdot \overline{P_{cutting}^0} \\ &= P_0 + f(\overline{VB}) \cdot \overline{P_{cutting}^0} \end{aligned} \tag{5}$$

where P (W) and P_0 (W) are the total powers with and without tool wear, respectively; $\overline{P_{cutting}}$ (W) and $\overline{P_{cutting}^0}$ (W) are the average cutting powers during one rotation period with and without tool wear, respectively. From Eq. (5), it can be observed the cutting force increase pattern is the same with the increase pattern of total power consumption versus initial cutting power. Therefore, $f(\overline{VB})$ can be estimated with the measured total power consumption, calculated initial cutting power, and tool wear. With the calibrated $f(\overline{VB})$, the explicit expression of the energy consumption model could be easily determined using Eq. (5).

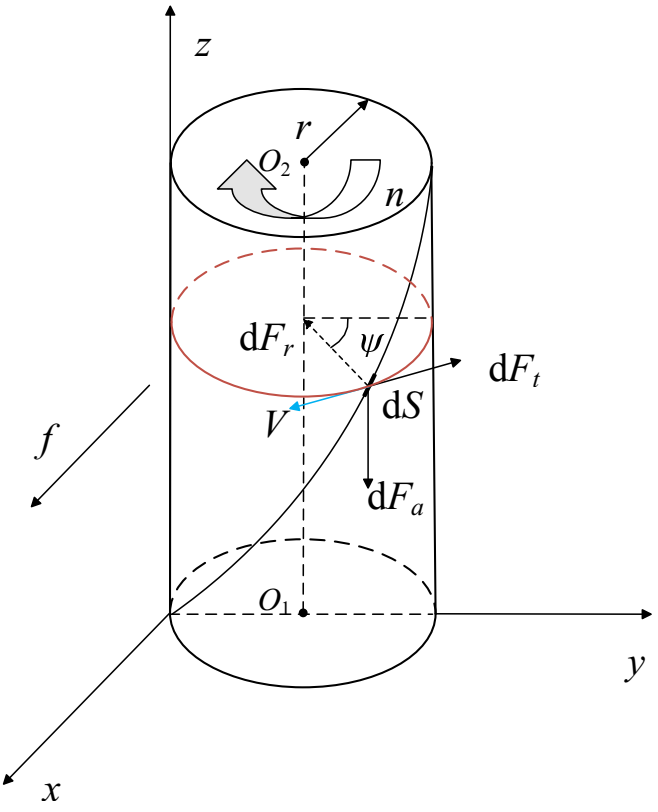

Fig. 1. A flat-end mill in slot milling process (Liu et al., 2015).

3. Experiment details for energy consumption model calibration and validation

In this study, a 3-axis CNC vertical milling centre, LEADWELL MCV-1500i+, was used to perform the milling experiments. Five 2-flute solid carbide flat-end mills, noted as Cutter-1 to Cutter-5, were used in this experiment. These cutters were made of the same material and manufactured in the same batch. Each cutter has a helix angle of 40° and a radius of 5 mm. Therefore, they can be considered identical in this experiment. Cutter-1 was used for calibrating cutting force coefficients in Experiment-I, while the other four cutters were used for tool wear-related experiments in Experiment-II. All the milling processes were performed under dry cutting conditions. During each tool setup, the cutter runout was sufficiently minimized and the hang length was kept at a constant

Table 1
Physical and mechanical properties of the used titanium alloy.

Major properties	Titanium alloy TC4
Density [g·cm^{-3}]	4.42
Thermal conductivity [W·m^{-1} K^{-1}]	7.2
Melting temperature [°C]	1649
Specific heat [J·kg^{-1} K^{-1}]	560
Elasticity modulus [GPa]	114
Yield strength [MPa]	880
Tensile strength [MPa]	950

Table 2
Parameter settings for Experiment-I.

No.	Milling cutter	Milling type	a_e [mm]	a_p [mm]	n [rpm]	f [mm/min]
1	**Cutter-1**	Slotting	10.0	1.0	2000.0	100.0
2		Slotting	10.0	2.0	2000.0	200.0
3		Up milling	2.0	2.0	1500.0	200.0
4		Down milling	2.0	2.0	1500.0	200.0

value of 35 mm. The workpiece material is titanium alloy Ti6Al4V (TC4), a type of alloy that is extensively used in aerospace industry. The major properties of TC4 alloy are provided in Table 1. The dimension of the workpiece is 144 mm × 100 mm × 20 mm.

In Experiment-I, Cutter-1 is firstly used for calibrating cutting force coefficients. The cutting conditions are presented in Table 2, where a_e, a_p, f and n are width of cut, depth of cut, feedrate and rotation speed, respectively. During Experiment-I, the cutting force profiles were collected with a 3-channel dynamometer (Kistler 9255B) at a sampling frequency of 20 kHz. The force signals were firstly amplified by a Kistler 5080 charge amplifier and then collected by a DEWE3010 digital collector. The setup of the dynamometer are shown in Fig. 2 (a) and (b). Setting-1 was used for calibration of cutting force coefficients, and the other three parameter settings were used to test the accuracy of the determined coefficients.

In Experiment-II, four sets of slotting experiments were performed according to cutting conditions in Table 3. The power profiles were measured during the whole experiments. They were

Table 3
Parameter settings for Experiment-II.

No.	Milling cutter	Milling type	a_e [mm]	a_p [mm]	n [rpm]	f [mm/min]
1	**Cutter-2**	Slotting	10.0	0.5	2000.0	300.0
2	**Cutter-3**	Slotting	10.0	0.5	1000.0	150.0
3	**Cutter-4**	Slotting	10.0	1.0	1000.0	300.0
4	**Cutter-5**	Slotting	10.0	1.0	2000.0	150.0

measured using a Panasonic Eco-Power Meter KW9M installed at the mains of the machine tool. Voltage signals via direct wiring and current signals via three current transformers are taken as input at the terminal blocks, as shown in Fig. 2 (c) and (d). The sampling frequency of power is 10 Hz. Under each parameter setting, a new cutter is used for slotting experiments. At each layer of the workpiece, nine slots were machined with each slot representing 100 mm cutting distance. Then, facing milling with an 80 mm end mill was performed to smooth the workpiece surface. The slotting experiments continued until the cutter reached a $\overline{VB}$ value of 300 μm. The $\overline{VB}$ values of Cutter-2 to Cutter-5 were measured using a microscope every 18 slots (i.e., slot-18, slot-36, slot-54 …). The setup of the microscope is shown in Fig. 2 (e). Setting-1 was used to calibrate the cutting force increase pattern as well as determine the energy consumption model with tool wear progression. The other three parameter settings were used to test the effectiveness of the proposed model in terms of the following two criteria, respectively:

(1) Power prediction from measured tool wear;
(2) Tool wear prediction from measured total power.

4. Results and discussions

In this section, the overall procedure for determining the proposed model is firstly demonstrated. To test the effectiveness of the calibrated model, prediction results of power and tool wear for cutting experiments under new cutting conditions are compared with the measured results.

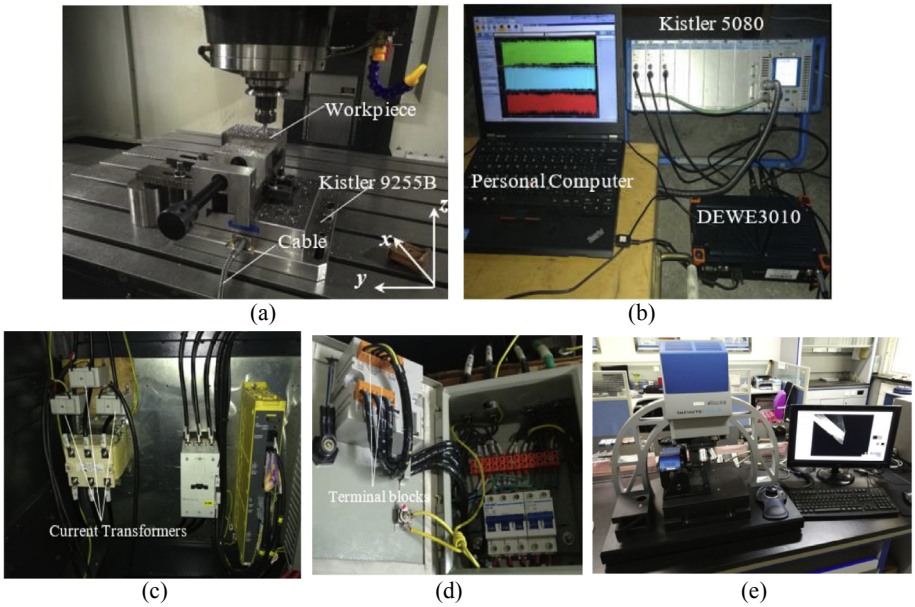

Fig. 2. The experiment setups. (a) and (b): Setup for cutting force measurement. (c) and (d): Setup for power measurement. (e): Setup for tool wear measurement.

4.1. Calibration of cutting force coefficients

The cutting force coefficients can be obtained from the database if they are previously calibrated. In this paper, they are calibrated through cutting experiments since they are not available in the existing database. The standard linear least squares (LLS) method was applied for the calibration of cutting force coefficients (Liu et al., 2016b; Wang et al., 2015). Using the measured cutting force profile from setting-1 in Experiment-I, the calculated cutting force coefficients is

$$\boldsymbol{K} = [K_{te}\ K_{tc}\ K_{re}\ K_{rc}]^T = [-28.8\ -2131.0\ -96.3\ 146.3]^T$$

K_{ae} and K_{ac} are not considered since they are not involved in cutting power calculation. To test the accuracy of the obtained cutting force coefficients, $\boldsymbol{K}$ was used to predict the cutting force along x-direction in the other parameter settings in Experiment-I. The results are shown in Fig. 3. As can be seen, although $\boldsymbol{K}$ was calculated from setting-1, the prediction results for the other parameter settings were generally acceptable. This guarantees the accuracy of the calculated cutter power.

4.2. Calibration of the polynomial coefficients

Setting-1 in Experiment-II is used for calibrating polynomial coefficients in Eq. (3). Tool wear measurement shows there is no abrupt tool breakage in the machining process. The relationship between total power consumption and tool wear is plotted in Fig. 4. It can be observed the power consumption does not suffer great changes at initial tool wear stage. As the slotting process continues, the power consumption increases steadily. At severe wear stage, a much higher increase rate of power can be observed. Based on the above observations, $f(\overline{VB})$ can be assumed to be second-order. Higher order is not considered here in case of over-fitting.

To calibrate $f(\overline{VB})$, P_0 and $\overline{P^0_{cutting}}$ are firstly measured and calculated, respectively. Denoting the number of points in Fig. 4 as M, $f(\overline{VB})$ can be calibrated using LLS method as

$$A = \left(W^T W\right)^{-1} W^T (P - P_0) \Big/ \overline{P^0_{cutting}} \tag{6}$$

Where $A = [a_1\ \ a_2\ \ \ldots\ \ a_N]^T$ and the i-th row of W is $W(i) = \left[\overline{VB}_i\ \ \overline{VB}_i^2\ \ \ldots\ \ \overline{VB}_i^N\right]$ with $i = 1, 2, \ldots M$; P contains the measured power values. Applying $N = 2$ since $f(\overline{VB})$ is second-order, A can be calibrated as

$$A = [a_1\ a_2] = \left[2.409 \times 10^{-3}\quad 5.866 \times 10^{-6}\right]^T \tag{7}$$

In order to test the parameter estimates in A, R-squared value and 95% confidence intervals ($\alpha = 0.05$) are computed (MathWorks, 2017), respectively. The results are shown in Table 4. As can be seen, the R-squared value is sufficiently close to 1, showing the quadratic model fits the data very well. It can also be found the parameter estimates in A are both located in 95% confidence intervals, indicating a high correlation between the data points and the obtained quadratic model.

With Eq. (7), $f(\overline{VB})$ can also be determined as

$$f(\overline{VB}) = 2.409 \times 10^{-3}\overline{VB} + 5.866 \times 10^{-6}\overline{VB}^2 \tag{8}$$

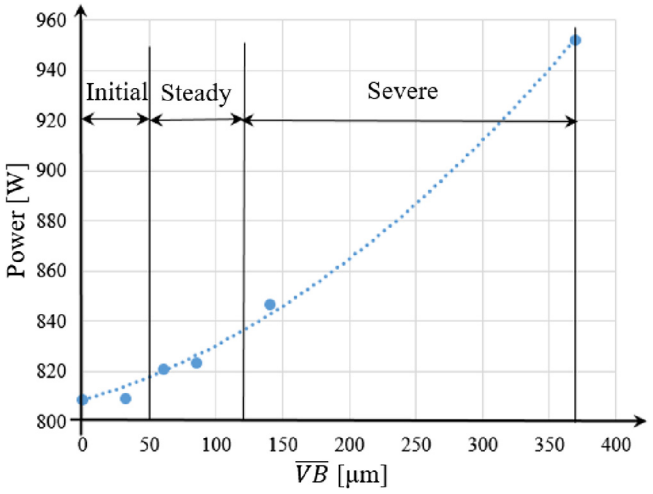

Fig. 4. Total power consumption versus measured tool wear.

Table 4
Obtained R-squared value and 95% confidence intervals for the parameter estimates.

Term	Value
R-squared	0.9947
Confidence interval for a_1	$[1.245 \times 10^{-3}, 3.573 \times 10^{-3}]$
Confidence interval for a_2	$[2.407 \times 10^{-6}, 9.325 \times 10^{-6}]$

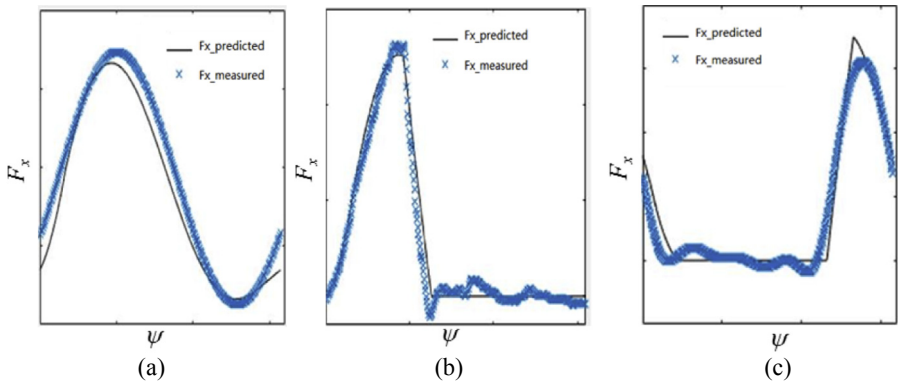

Fig. 3. Cutting force prediction under new cutting conditions. (a): Slotting experiment with setting-2 in Experiment-I. (b): Slotting experiment with setting-3 in Experiment-I. (c): Slotting experiment with setting-4 in Experiment-I.

The total power consumption model with tool wear progression can be obtained as

$$P^* = P_0 + f(\overline{VB}) \cdot \overline{P^0_{cutting}} = P_0 + \left(2.409 \times 10^{-3}\overline{VB} + 5.866 \times 10^{-6}\overline{VB}^2\right) \cdot \overline{P^0_{cutting}} \quad (9)$$

where P^* represents the predicted power consumption at a given $\overline{VB}$.

So far, the whole procedure for the calibration of the proposed model has been demonstrated. There are four steps in total and can be generally described as follows:

(1) Determine the cutting force coefficients with the current tool-workpiece couple. The coefficients can either be obtained from existing database or calculated through cutting experiments.
(2) Estimate the shape of the cutting force increase pattern, $f(\overline{VB})$. This can be done through cutting experiments using a new cutter.
(3) Calibrate the involved coefficients with using Eq. (6).
(4) Determine the explicit power consumption model with Eq. (5).

Using the calibrated model, energy consumption under a certain tool wear condition can be predicted. Vice versa, the tool wear condition can also be estimated with measured power consumption since the tool wear and power consumption exhibits a one-to-one correspondence.

4.3. Model validation for power consumption prediction

The measured results of tool wear and power consumption in the other parameter settings of Experiment-II are shown in Table 5. P_2, P_3 and P_4 represent measured power consumption values when milling the current slot. They were obtained by averaging the power readings over a period of 10 s in steady slotting states (i.e., excluding cutter entry and exit). The measured tool wear values of these parameter settings are shown under column $\overline{VB}_2$, $\overline{VB}_3$ and $\overline{VB}_4$, respectively. Power values of slot-1 were also recorded and they are considered as the power consumption of new cutter without tool wear (P_0). The average cutting power without tool wear is shown in the last row of Table 5. They were calculated using the calibrated $\boldsymbol{K}$ in Section 4.1 and the parameter settings.

With the measured P_0 and calculated $\overline{P^0_{cutting}}$, the power consumption can be predicted using Eq. (7). The predicted power consumption results from tool wear is shown Table 6, where P_i^* and E_i ($i = 2, 3, 4$) are the predicted power and relative prediction error, respectively. The relative prediction error is calculated using $E_i = \left|P_i^* - P_i\right|/P_i \times 100\%$.

The predicted results and measured results are visualized in Fig. 5. As can be seen, the power consumption generally increases as tool wear propagates. This is due to the additional cutting forces caused by the wear lands. Moreover, it can be observed that the predicted power consumption agrees well with the measured power consumption in all the three parameter settings. As can be seen from the last row of Table 6, the relative prediction errors are only around 1%, despite of the changing cutting conditions. This clearly shows the effectiveness of the proposed model for prediction power consumption with tool wear progression.

Table 5
Measured results in parameter setting-2, setting-3 and setting-4 in Experiment-II.

Slot no.	$\overline{VB}_2$ [μm]	P_2 [W]	$\overline{VB}_3$ [μm]	P_3 [W]	$\overline{VB}_4$ [μm]	P_4 [W]
1	0.0	583.6	0.0	733.0	0.0	790.2
18	22.9	590.3	45.2	753.8	40.4	795.0
36	34.4	592.2	63.0	758.1	53.2	795.8
54	46.8	594.3	93.5	775.5	66.8	803.3
72	52.2	589.4	122.7	782.8	76.6	809.8
90	63.5	593.2	166.0	795.0	83.5	817.0
108	88.3	595.2	185.9	801.4	105.7	824.7
126	110.2	602.7	203.6	808.6	122.0	834.2
144	140.1	610.9	211.0	837.1	140.4	852.3
162	215.0	623.6	226.9	842.0	197.2	865.7
180	240.5	628.5	237.1	867.4	423.2	978.1
198	262.7	635.8	323.4	913.1		
216	336.7	647.5				
$\overline{P^0_{cutting}}$ [W]		**36.6**		**126.7**		**92.9**

4.4. Model validation for tool wear prediction

With the proposed energy consumption model, the tool condition can also be monitored. With P_0 and $\overline{P^0_{cutting}}$, $\overline{VB}$ can be easily estimated by solving Eq. (9) using the power data shown in Table 5. Similarly, the predicted results and the visualized comparative results are provided in Table 7 and Fig. 6, respectively. In Table 7, $\overline{VB}_i^*$ and $\Delta\overline{VB}_i$ ($i = 2, 3, 4$) are the predicted tool wear and absolute tool wear error ($\Delta\overline{VB}_i = \left|\overline{VB}_i^* - \overline{VB}_i\right|$), respectively.

As can be seen from Fig. 6 (b) and (c), the prediction results

Table 6
Predicted power results for setting-2, setting-3 and setting-4 in Experiment-II.

Slot no.	P_2^* [W]	E_2	P_3^* [W]	E_3	P_4^* [W]	E_4
18	585.7	0.8%	748.3	0.7%	799.9	0.6%
36	586.8	0.9%	755.2	0.4%	803.4	1.0%
54	588.2	1.0%	768.0	1.0%	807.4	0.5%
72	588.7	0.0%	781.6	0.1%	810.3	0.2%
90	590.0	0.5%	804.1	1.2%	812.5	0.6%
108	593.0	0.4%	815.4	1.8%	819.7	0.5%
126	595.9	1.1%	826.0	2.1%	825.4	1.1%
144	600.1	1.8%	830.5	0.8%	832.2	2.4%
162	612.4	1.8%	840.6	0.2%	855.3	1.1%
180	617.2	1.8%	847.1	2.3%	982.3	0.4%
198	621.5	2.2%	909.5	0.4%		
216	637.6	1.5%				
Average error		1.2%		1.0%		0.8%

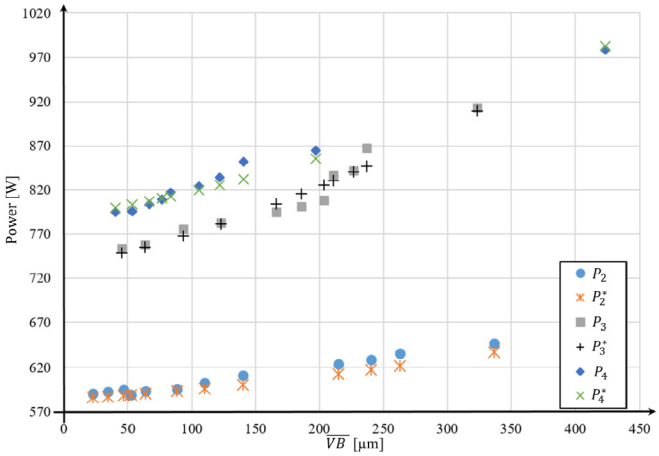

Fig. 5. Predicted power consumption with tool wear versus measured power consumption.

Table 7
Predicted tool wear for setting-2, setting-3 and setting-4 in Experiment-II.

Slot no.	$\overline{VB}_2^*$ [μm]	$\Delta\overline{VB}_2$ [μm]	$\overline{VB}_3^*$ [μm]	$\Delta\overline{VB}_3$ [μm]	$\overline{VB}_4^*$ [μm]	$\Delta\overline{VB}_4$ [μm]
18	65.9	43.0	59.5	14.3	21.2	19.2
36	81.8	47.4	70.3	7.3	24.5	28.7
54	97.6	50.8	109.8	16.3	52.8	14.1
72	54.5	2.3	125.0	2.3	72.2	4.4
90	89.8	26.3	149.0	17.0	97.6	14.1
108	105.2	16.9	160.9	25.0	118.0	12.4
126	157.1	46.9	174.0	29.6	145.8	23.7
144	206.4	66.4	221.6	10.6	190.3	49.8
162	272.9	57.9	229.1	2.2	219.2	22.0
180	296.2	55.7	266.9	29.8	417.1	6.2
198	329.0	66.3	328.0	4.5		
216	377.8	41.1				
Average $\Delta\overline{VB}$ [μm]	**43.4**		**14.4**		**19.5**	

demonstrate a good agreement with the measured values in setting-3 and setting-4. The average absolute prediction errors are both smaller than 20 μm. This shows the proposed model can be used as an accurate tool wear estimation method. However, it is also noticed that the predicted results for setting-2 ($\Delta\overline{VB}_2$ = 43.4 μm) are not as accurate as the other two settings. In addition, as can be seen from Table 5, the measured powers of the first 108 slots are almost the same. In slot-72, the power consumption even became lower than before. A possible explanation can be found in Fig. 7. As can be seen, the cutter with setting-2 suffers much more significant tool breakage than other cutters. As a result, the total number of effective infinitesimal cutting edges may be reduced in the initial wear state. Therefore, there may be possible decrease of the required power consumption due to decreased cutting force. In this case, the accuracy of the proposed model will be affected since the cutting force increase pattern will change due to abrupt tool

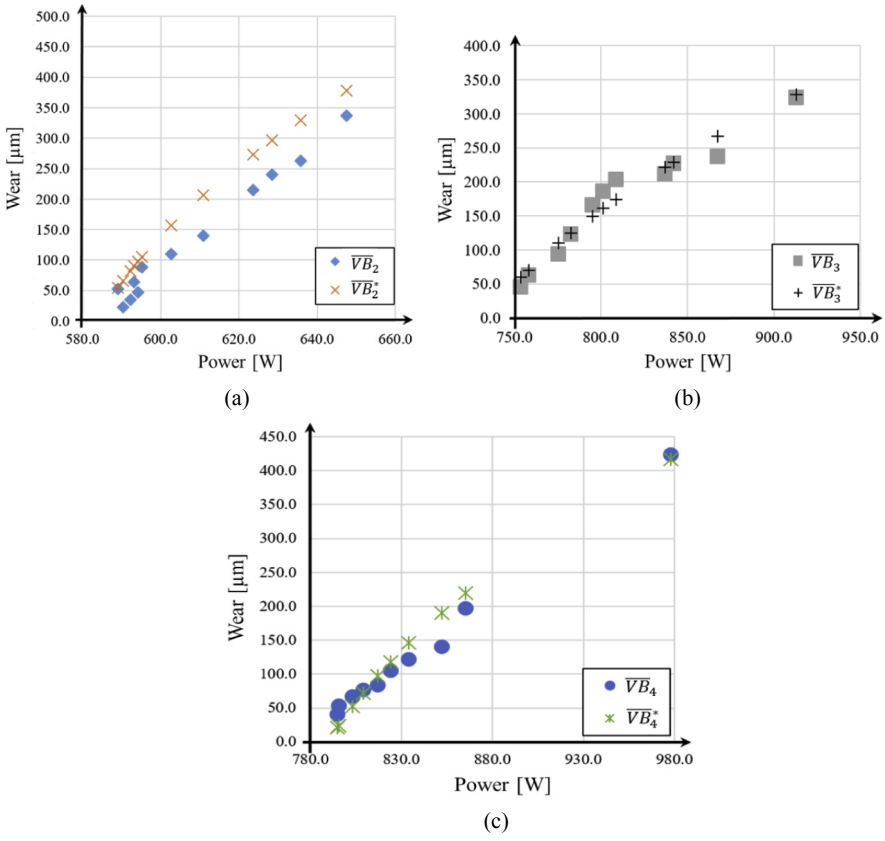

Fig. 6. Predicted tool wear with tool wear versus measured tool wear. (a): Setting-2 in Experiment-II. (b): Setting-3 in Experiment-II. (c): Setting-4 in Experiment-II.

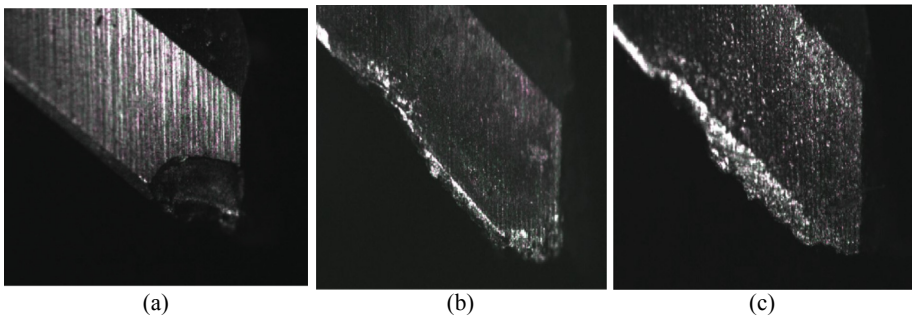

Fig. 7. Tool wear measurement of cutters in Experiment-II. (a): Tool wear after slot-108 with setting-2. (b): Tool wear after slot-108 with setting-3. (c): Tool wear after slot-108 with setting-4.

breakage. Nonetheless, the predicted trend shows an acceptable agreement with the measured one. Besides, the prediction accuracy actually increases as $\overline{VB}$ gets larger. In this sense, the proposed method can still be used as a rough estimation method when abrupt tool breakage happens.

Compared with other monitoring methods such as acoustic emission and vibration, this tool wear estimation method does not require expensive measurement equipment or complicated setup. The cutting force coefficients can be easily found in the existing database and the power signal is easy to measure with a power meter. With only one calibration, the proposed model is able to provide reliable predictions for new cutting conditions as long as the tool-workpiece couple remains unchanged. Therefore, this tool wear estimation method is not only straightforward but also cost-effective.

5. Conclusions

Energy consumption models are of great importance to energy-efficient manufacturing since it offers the fundamental basis for optimizing energy efficiency. In machining process, tool wear is inevitable due to interaction between the tool tip and workpiece material. Traditional energy consumption models fail to take this important factor into consideration. To address this issue, this study aims to propose a reliable energy consumption model with tool wear progression for 3-axis milling process. It was firstly derived from modern machining theory and a hybrid energy consumption model. Subsequently, the proposed model is calibrated from cutting experiments. The comparison results show that the proposed energy consumption model is able to provide reliable power prediction results under new cutting conditions. As such, the proposed model can be a valuable supplement to energy consumption modelling in machining process, and may provide a more comprehensive platform in energy efficiency optimization. In addition, the calibrated model can also serve as an effective platform for tool wear estimation from power consumption. Compared with other monitoring methods such as acoustic emission and vibration, this tool wear estimation method is not only straightforward but also cost-effective.

As long as the tool-workpiece couple remains the same, the proposed model is expected to provide reliable prediction results regardless of cutting conditions. However, the cutting force increase pattern ($f(\overline{VB})$) may vary from different combinations of tool and workpiece. The next stage of this study will explore the relationship between f ($\overline{VB}$) and tool-workpiece couple. Besides, energy-efficient process planning based on the proposed energy consumption model will be carried out.

Acknowledgements

This study was supported by the National Natural Science Foundation of China (grant number 51775444 & No. 51375508). The authors would like to acknowledge this financial support.

The authors also want to give special thanks to Prof. YUAN Yuan for her advice on the statistical analysis.

References

Balogun, V.A., Mativenga, P.T., 2014. Impact of un-deformed chip thickness on specific energy in mechanical machining processes. J. Clean. Prod. 69, 260–268. https://doi.org/10.1016/j.jclepro.2014.01.036.

Budak, E., Altintas, Y., Armarego, E.J.A., 1996. Prediction of milling force coefficients from orthogonal cutting data. J. Manuf. Sci. Eng. 118, 216–224. https://doi.org/10.1115/1.2831014.

Bunse, K., Vodicka, M., Schönsleben, P., Brülhart, M., Ernst, F.O., 2011. Integrating energy efficiency performance in production management - gap analysis between industrial needs and scientific literature. J. Clean. Prod. 19, 667–679. https://doi.org/10.1016/j.jclepro.2010.11.011.

Cai, W., Liu, F., Xie, J., Liu, P., Tuo, J., 2017. A tool for assessing the energy demand and efficiency of machining systems : energy benchmarking. Energy 138, 332–347. https://doi.org/10.1016/j.energy.2017.07.039.

Diaz, N., Redelsheimer, E., Dornfeld, D., 2011. Energy consumption characterization and reduction strategies for milling machine tool use. Glocalized Solut. Sustain. Manuf. 263–267. https://doi.org/10.1007/978-3-642-19692-8_46.

Guo, Y., Loenders, J., Duflou, J., Lauwers, B., 2012. Optimization of energy consumption and surface quality in finish turning. Proc. CIRP 1, 512–517. https://doi.org/10.1016/j.procir.2012.04.091.

Gutowski, T., Dahmus, J., 2007. A thermodynamic characterization of manufacturing processes. In: Electron. Environ. Proc. 2007 IEEE Int. Symp, pp. 137–142. https://doi.org/10.1109/ISEE.2007.369382.

Gutowski, T., Dahmus, J., Thiriez, A., 2006. Electrical energy requirements for manufacturing processes. In: 13th CIRP Int. Conf. life cycle Eng, 31, pp. 623–638.

Hou, Y., Zhang, D., Wu, B., Luo, M., 2015. Milling force modeling of worn tool and tool flank wear recognition in end milling. IEEE/ASME Trans. Mechatron. 20, 1024–1035. https://doi.org/10.1109/TMECH.2014.2363166.

Kara, S., Li, W., 2011. Unit process energy consumption models for material removal processes. CIRP Ann. Manuf. Technol. 60, 37–40. https://doi.org/10.1016/j.cirp.2011.03.018.

Kuram, E., Ozcelik, B., Bayramoglu, M., Demirbas, E., Simsek, B.T., 2013. Optimization of cutting fluids and cutting parameters during end milling by using D-optimal design of experiments. J. Clean. Prod. 42, 159–166. https://doi.org/10.1016/j.jclepro.2012.11.003.

Lee, P., Altintas, Y., 1996. Prediction of ball-end milling forces from orthogonal cutting data. Int. J. Mach. Tools Manuf. 36, 1059–1072. https://doi.org/10.1016/0890-6955(95)00081-X.

Li, C., Chen, X., Tang, Y., Li, L., 2017. Selection of optimum parameters in multi-pass face milling for maximum energy efficiency and minimum production cost. J. Clean. Prod. 140, 1805–1818. https://doi.org/10.1016/j.jclepro.2016.07.086.

Li, L., Yan, J., Xing, Z., 2013. Energy requirements evaluation of milling machines based on thermal equilibrium and empirical modelling. J. Clean. Prod. 52, 113–121. https://doi.org/10.1016/j.jclepro.2013.02.039.

Li, W., Kara, S., 2011. An empirical model for predicting energy consumption of manufacturing processes: a case of turning process. Proc. Inst. Mech. Eng. Part B J. Eng. Manuf. 225, 1636–1646. https://doi.org/10.1177/2041297511398541.

Liu, N., Wang, S.B., Zhang, Y.F., Lu, W.F., 2016b. A novel approach to predicting surface roughness based on specific cutting energy consumption when slot milling Al-7075. Int. J. Mech. Sci. 118, 13–20. https://doi.org/10.1016/j.ijmecsci.2016.09.002.

Liu, N., Zhang, Y.F., Lu, W.F., 2015. A hybrid approach to energy consumption modelling based on cutting power: a milling case. J. Clean. Prod. 104, 264–272. https://doi.org/10.1016/j.jclepro.2015.05.049.

Liu, Z., Guo, Y., Sealy, M.P., Liu, Z., 2016a. Energy consumption and process sustainability of hard milling with tool wear progression. J. Mater. Process. Technol. 229, 305–312. https://doi.org/10.1016/j.jmatprotec.2015.09.032.

Luo, M., Luo, H., Zhang, D., Tang, K., 2017. Improving tool life in multi-axis milling of Ni-based superalloy with ball-end cutter based on the active cutting edge shift strategy. J. Mater. Process. Technol. 252, 105–115. https://doi.org/10.1016/j.jmatprotec.2017.09.010.

MathWorks, 2017. nlparci:Nonlinear Regression Parameter Confidence Intervals [WWW Document]. URL. https://www.mathworks.com/help/stats/nlparci.html.

Park, C., Kwon, K., Kim, W., Min, B., 2009. Energy consumption reduction technology in manufacturing—A selective review of policies, standards, and research. Int. J. Precis. Eng. Manuf. 10, 151–173. https://doi.org/10.1007/s12541-009-0107-z.

Sealy, M.P., Liu, Z.Y., Zhang, D., Guo, Y.B., Liu, Z.Q., 2015. Energy consumption and modeling in precision hard milling. J. Clean. Prod. 1–11. https://doi.org/10.1016/j.jclepro.2015.10.094.

Shao, H., Wang, H.L., Zhao, X.M., 2004. A cutting power model for tool wear monitoring in milling. Int. J. Mach. Tools Manuf. 44, 1503–1509. https://doi.org/10.1016/j.ijmachtools.2004.05.003.

Sun, Y., Sun, J., Li, J., Li, W., Feng, B., 2013. Modeling of cutting force under the tool flank wear effect in end milling Ti6Al4V with solid carbide tool. Int. J. Adv. Manuf. Technol. 69, 2545–2553. https://doi.org/10.1007/s00170-013-5228-y.

Waldorf, D.J., Kapoor, S.G., DeVor, R.E., 1992. Automatic recognition of tool wear on a face mill using a mechanistic modeling approach. Wear 157, 305–323. https://doi.org/10.1016/0043-1648(92)90069-K.

Wang, S.B., Geng, L., Zhang, Y.F., Liu, K., Ng, T.E., 2015. Cutting force prediction for five-axis ball-end milling considering cutter vibrations and run-out. Int. J. Mech. Sci. 96, 206–215. https://doi.org/10.1016/j.ijmecsci.2015.04.007.

Yoon, H., Lee, J., Kim, M., Ahn, S., 2014. Empirical power-consumption model for material removal in three- axis milling. J. Clean. Prod. 78, 54–62. https://doi.org/10.1016/j.jclepro.2014.03.061.